Experimental characterization of retention properties and microstructure of the Czech bentonite B75

Caractérisation expérimentale des propriétés de rétention et de la microstructure de la bentonite tchèque B75

Haiquan Sun & David Mašín* & Jan Boháč
Faculty of Science, Charles University, Czech Republic, (*seaspringsun@gmail.com*)

ABSTRACT: In this paper, water retention curves of compacted Czech bentonite B75 measured by vapour equilibrium methods are presented. The controlled suction range was 3.29 MPa-286.7 MPa. The changes in microstructure of compacted bentonite under free swelling was studied upon wetting and drying path. Mercury intrusion porosimetry (MIP) and environmental scanning electron microscope (ESEM) were used for the microstructure observation. The MIP tests were performed on samples with two initial dry densities at three different suction levels. The ESEM observations were performed on the same samples, while the target relative humidity is imposed directly in ESEM chamber. The ESEM and MIP results clarified the microstructural changes which bentonite undergoes during wetting and drying process. Interestingly, it appears that the aggregates are relatively insensitive to suction changes and significant proportion of wetting-induced swelling occurs on the macrostructure level. We indirectly observed that the microstructure desaturated during drying and it thus appears that the common assumption of saturated microstructure may not be accurate.

RÉSUMÉ : Dans cet article, nous présentons les courbes de rétention d'eau de la bentonite tchèque compacte B75 mesurée par des méthodes d'équilibre de vapeur. La plage d'aspiration contrôlée est de 3,29 MPa à 286,7 MPa. Les modifications de la microstructure de la bentonite compacte sous gonflement libre sont étudiées lors du mouillage et du séchage. Pour l'observation de la microstructure, on utilise la porosimétrie à intrusion de mercure (MIP) et le microscope électronique à balayage environnemental (ESEM). Les tests MIP ont été effectués sur des échantillons avec deux densités initiales à trois niveaux d'aspiration différents. Les observations ESEM sont effectuées sur les mêmes échantillons, tandis que l'humidité relative cible est imposée directement dans la chambre ESEM. Les résultats ESEM et MIP clarifient les changements micro-structuraux subis par la bentonite lors du mouillage et du séchage. Il est intéressant de noter que les agrégats sont relativement insensibles aux changements d'aspiration et qu'une proportion importante du gonflement induit par mouillage se produit au niveau de la macro-structure. Nous observons indirectement que la microstructure désaturait pendant le séchage et il apparaît ainsi que l'hypothèse commune de la microstructure saturée peut ne pas être précise.

KEYWORDS: bentonite, microstructure, MIP, ESEM

1 INTRODUCTION

The Czech Radioactive Waste Repository Authority (SURAO) is currently considering the Czech compacted bentonite B75 as a potential engineered barrier material for a Czech Republic high level nuclear waste disposal. The characteristics of the compacted bentonite B75 must be investigated and evaluated by laboratory experiments and in situ tests. In thispaper, we focus on the microstructure and water retention properties of the B75 bentonite.

Bentonite is not only used in many industries as a suspending and stabilization agent, but is also planned extensively as a buffer in engineered barriers of high level nuclear waste disposal (Push 1982). The experimental and constitutive behaviour of bentonite has been studied by many researchers (Gens & Alonso 1992; Alonso 1998; Delage et al., 1996; Alonso, 2010; Mašín 2013). They pointed out that the behaviour of this kind material is quite complex, because it results from the volume change of the aggregates and their skeleton rearrangement (macrostructure) and the physical-chemical interaction of clay minerals within the aggregates (microstructure). It is assumed that the microstructural deformation behaviour is fully reversible and not affected by the state of the macrostructure (Gens & Alonso, 1992). This assumption was adopted by Mašín (2013) in his double structure model. In contrast, the macropores will desaturate/saturate by increasing/decreasing suction and its behavior may be, in fact, described by conventional frameworks for unsaturated soils. Although the behaviour of the microstructure is expected to be independent of the macrostructure, there is an important influence of the microstructure on the macrostructural behaviour, where it can induce significant plastic strains. The magnitude of the interaction depends on the current stress state and on the density of the macrostructure (Lloret et al. 2003).

2 MATERIAL AND METHODS

The commercial compacted Czech bentonite B75 extracted from the Cerny vrch deposit (north-western region of the Czech Republic), was used in this study. It is a calcium-magnesium bentonite with a montmorillonite content of around 60% and initial water content about 10%. Table 1 lists its physical parameters. The plastic limit, liquid limit and specific gravity of solid soils are 65%, 229%, and 2.87, respectively. The cation exchange capacity is shown in Table 2.

Table 1. Physical properties of bentonite B75 (Stastka et al., 2015).

Property	Description
Montmorillonite (%)	60
Liquid limit (%)	229
Plastic limit (%)	65
Plasticity index Ip	164
Particle density ρs (g/cm3)	2.87

Table 2. The cation exchange capacity of bentonite B75.

Cation	mmol/100g
Ca^{2+}	36.92
Na^+	65.75
K^+	3.03
Mg^{2+}	26.84
H^+	<0.5

Water retention curve measurements were performed in the following way. The samples of three different initial dry densities were cut into irregular pieces weighing 0,8-1,5 g and dried in the oven at 110°C for more than 48 hours. Half of the samples were tested directly under wetting path, the other half was equilibrated at 3.29 MPa using vapour equilibrium method and tested under drying path. Finally, water content, void ratio and degree of saturation were measured at each of the samples. Table 3 shows the salt solution used for vapour equilibrium method measurements.

Table 3. Salt used for vapour equilibrium method measurements (constant temperature 20 °C) (OIML, 1996)

Salt solutions	Solubility (g/100ml)	Relative humidity (%)	Suction (MPa)
$LiCl \cdot H_2O$	82.78	12.0	286.7
CH_3COOK	268.6	23.1	198.14
$MgCl_2 \cdot 6H_2O$	55.24	33.1	149.51
K_2CO_3	109.43	43.2	113.50
$NaBr$	91.21	59.1	71.12
$NaCl$	36	75.5	38.00
KCl	34	85.1	21.82
K_2SO_4	11.05	97.6	3.29

MIP tests were performed at the Department of Inorganic Technology at the University of Chemistry and Technology Prague (Apparatus Autopore IV, Micromeritics). The samples of two different initial dry densities were equilibrated at suctions of 286.7 MPa, 38 MPa and 3.29 MPa. The samples were then freeze-dried to preserve their microstructure and tested under the mercury pressures between 0.01 MPa (0.1 mm pore radius) and 400 MPa (1.5 nm pore radius).

The Environmental Scanning Electron Microscope tests have been performed using QUANTA 650 FEG scanning electron microscope at the Institute of Scientific Instruments of the Czech Academy of Sciences, Brno. The samples equilibrated at the suction of 286.7MPa were used for ESEM observations. The samples taken from the desiccator have immediately been prepared for the ESEM test. The tests were performed at constant temperature of 5°C, the water vapour pressure was imposed directly in the ESEM chamber, which allowed us to observe directly the microstructure response to suction changes. The water vapour pressure of 93 Pa (relative humidity of 10%) were determined as optimal initial conditions for the experiment. Then the vapour pressure was gradually increased up to 850 Pa (the relative humidity 97%). After the maximum value of the relative humidity was reached, the relative humidity was gradually decreased again down to 10%. The interval between vapour pressure changes was 15 minutes.

3 RESULTS AND DISCUSSION

3.1 *Water transient phase*

The water content changes with time along wetting path are shown in Figure 1. The samples were tested at three different initial dry densities (1.27 Mg/m³, 1.6 Mg/m³ and 1.8 Mg/m³). For suctions 113.5 MPa to 286.7 MPa, water content increased quickly and then fluctuated along for a few days before it stabilised. The samples at 21.82 MPa to 71.82 MPa reached relatively quickly their stable states. Only the sample at the lowest suction of 3.29 MPa needed much longer time to equilibrate its water content (almost four months).
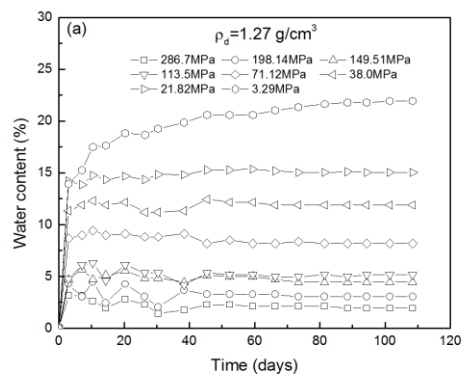
Figure 1. Water content vs. time for compacted bentonite B75 of initial dry density of 1.27 Mg/m³

3.2 *Water retention curves*

Figure 2(a) shows water content changes with suction of samples at three initial dry densities (wetting path). It is clear that the initial dry density had little influence on the water content, which increases linearly with logarithm of suction. Much more significant is the effect of suction on void ratio (Figure 2b). As most water is in the micropores at high suctions, these results suggest that suction affects predominantly macropores during water retention curve testing. Figure 2(c) shows the relationship between degree of saturation and suction. It is affected by the dry density substantially, but not due to the effect of water content, which is more or less the same at the three dry densities, but due to the effect of different void ratio.
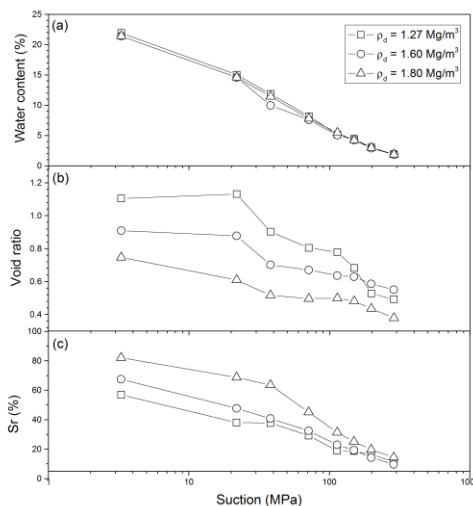
Figure 2. Water content (a), void ratio (b) and degree of saturation (c) versus suction for water retention curve measurements under wetting path at three different dry densities.

3.3 *MIP tests*

Figure 3 shows the mercury intrusion porosimetry results of low density (1.27 Mg/m³) samples at each suction level. It is clear that suction affects mainly the largest macropores (more than 2 μm in size) and smaller pores are less affected, although results are quite scattered for pores smaller than 0.1 μm. Results of

equivalent test at high initial dry density of 1.9 Mg/m³ are shown in Figure 4. In this case, macropores are substantially affected by suction (all pore sizes above 1 μm). In this case, also the pores below 1 μm are affected. It seems that proportion of pores up to 0.4 μm is invariable with suction, but the proportion of bigger pores increases with suction decrease.

The results of MIP testing are consistent with water retention curve measurements. Contrary to the expected behaviour, it seems that the smallest micropores are only marginally influenced by the suction value, and only larger pores above 0.4 μm contribute to wetting-induced swelling.

3 .3 *ESEM observation*

Figure 5 shows the ESEM micrographs of the compacted bentonite with a dry density of 1.27 Mg/m³ which was equilibrated at the total suction of 286.7 MPa. The arrangement of aggregates may be clearly seen, along with two different pore families (macropores and micropores). The aggregates are clearly visible in the smalles magnification picture, Zoom 2 and Zoom 3 then show details of the microstructure.
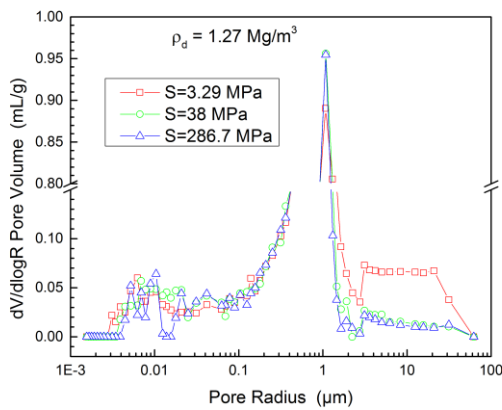
Fig 3. Pore density function curves of initial dry density of 1.27 Mg/m³ at three suction level
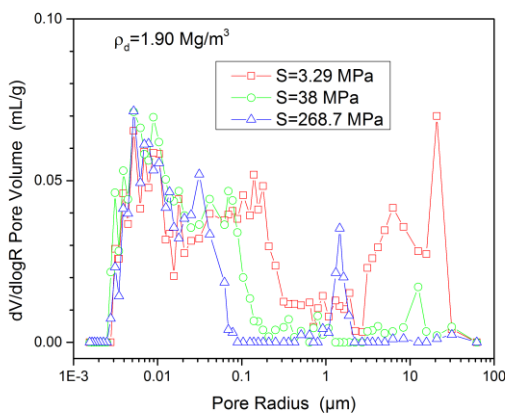
Figure 4. Pore density function curves of initial dry density of 1.90 Mg/m³ at three suction level

The micrographs of compacted bentonite upon wetting and drying are presented in Figure 6 for dry density of 1.27 Mg/m3. The double arrow is indicating the distance between selected aggregates. The distinctive macrostructural changes with changing suction can clearly be observed, irrespective of the fact that macrostructure remains dry up to relative humidities of 97%. It is clear that the macropore diameter increases upon wetting and decrease upon drying. We could also observe hysteretic

phenomenon occuring after one wetting-drying cycle. The aggregate distance was larger after wetting-drying cycle than initially.
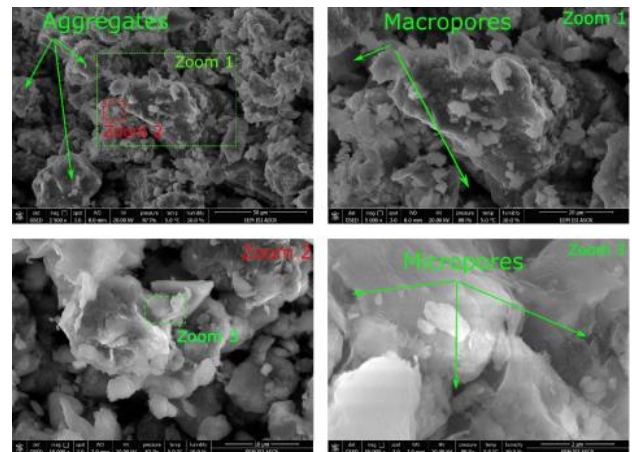
Figure 5. ESEM micrographs of compacted bentonite with a dry density of 1.27 Mg/m³ at different magifications.
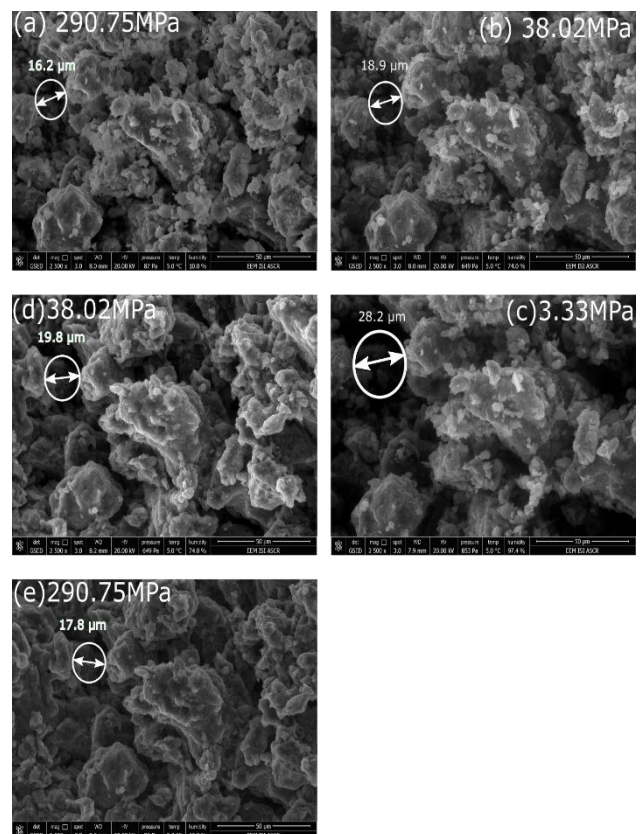
Figure 6. Selected ESEM micrographs of compacted bentonite with a dry density of 1.27 Mg/m³ under the wetting-drying path. (a),(b),(c)-wetting path; (c),(d),(e)-drying path.

During wetting, not only the aggregate distance changes, but also the aggregates themselves swell. In order to quantitatively analyse the volume change upon wetting and drying, the digital image analysis technique was used. The original ESEM photo represents a plan view in two-dimensions, as shown in Figure 7(a). Firstly, the original ESEM photos were adjusted by threshold grey level to clearly identify the boundary of the aggregates. Then, the surface area of the aggregate was measured using a software tool at each stage (see Figures 7(b-d)). The

surface strain is used to define the relative surface change of the aggregate plan view, defined as

$$\varepsilon = (S_i - S_0)/S_0 \times 100\% \qquad (1)$$

where ε is the surface strain, S_i is the surface area of the aggregate at the stage i, S_0 is the surface area of the aggregate at the initial state.

The surface strain upon wetting and drying path is shown in Figure 8. The surface strain increased with the increase of relative humidity, however, this increase is relatively minor up to the high humidity of 97%. There is a sudden increase in surface strain at the humidity of 97.4%, but we presume the values are affected by water entering the macropores which caused the aggregate boundaries to be less cleraly defined at the macrograph. During wetting, water remains initially in the macropores due to hydraulic hysteresis and thus also the aggregate surface area is appearing to be large. Below relative humidity of 75% the aggregate size appears to be insensitive to the hydraulic path and only very small effect of hydraulic hysteresis is measured: aggregate volumetric response thus appears to be reversible.

As both ESEM and MIP tests suggest that the aggregate size is relatively insensitive to suction, all water is within aggregates, but water content changes during drying are still remarkable (see results of WRC measurements), it appears that the microstructure desaturates quite significantly during drying proces, which opposes common assumption of saturated microstructure.
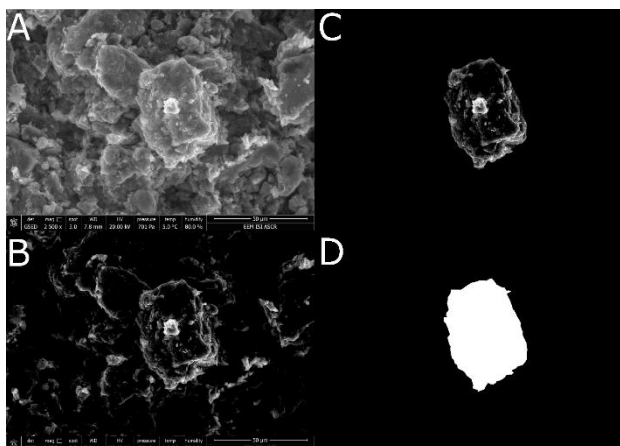
Figure 7. Digital image analysis methodology for target aggregates, (A) original ESEM microphotographs, (b) Image grey level adjustment, (c) target aggregates, (d) measurement the surface area.
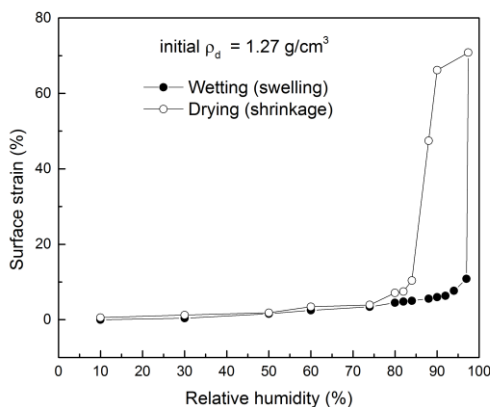
Figure.8 Surface strain versus relative humidity for compacted bentonite along wetting and drying path, sample with initial dry density of 1.27

Mg/cm³. At high relative humidities, results are affected by water entering the macropores.

4 CONCLUSION

In the paper, we presented results of water retention curves, MIP tests and ESEM micrographs of the Czech B75 bentonite at various initial dry densities. All the three experimental methods consistently show that the larger pores, which remain dry at higher suctions, contribute significantly to wetting-induced swelling. It also appears that aggregates desaturate remarkably during drying and thus the often assumed hypothesis of fully saturated microstructure may not be accurate.

5 ACKNOWLEDGEMENTS

6 REFERENCES

Alonso, E. E. 1988. keynote lecture: modelling expansive soil behavior. *Proc. 2nd Int. Conf. on Unsaturated Soils, Beijing* 1, 37-70

Alonso, E. E. et al. 2010 A microstructurally based effective stress for unsaturated soils *Géotechnique,* 60, No. 12, 913–925

Delage, P., Audiguier, M., Cui, Y. J. and Howat, M. D. 1996. Microstructure of a compacted silt. *Canadian Geotechnical Journal.* 33, 150-158

Gens, A. and Alonso, E. E. 1992. A framework for the behaviour of unsaturated clays. *Canadian Geotechnical Journal.* 29, 1013-1032

Stastka, J. and Smutek, J. 2015. Experimental works with bentonite pellets at the CEG. *LUCOEX Conference and workshop – Full-scale demonstration tests in technology development of repositories for disposal of radioactive waste. Oskarshamn, Sweden*. pp. 179-184

Lloret A., Villar M.V., Sánchez M., Gens A., Pintado X., Alonso E.E. Mechanical behaviour of heavily compacted bentonite under high suction changes. *Géotechnique,* 53 (1) (2003), pp. 27–40

Mašín D. Double structure hydromechanical coupling formalism and a model for unsaturated expansive clays. *Engineering Geology* 2013; 165:73–88.

The International Organization of Legal Metrology (OIML). 1996. The scale of relative humidity (RH) of air certified against saturated salt solutions. OIMLR 121, France.

Push R. 1982. Mineral-water interactions and their influence on the physical behavior of highly compacted Na-bentonite. *Canadian Geotechnical Journal,* 19 (3): 381–387.

Romero E. and Vaunat J. 2000. Retention curves of deformable clays. A. Tarantino, C. Mancuso (Eds.), *Experimental evidence and theoretical approaches in unsaturated soils. Proceedings of an international workshop on unsaturated soils, A.A. Balkema, Rotterdam, Netherlands,* pp. 91–106